

Hierarchical $\text{Mo}_x\text{C} @ \text{NC}$ Hollow Microsphere with Incorporated Mo Vacancies as Multifunctional Confined Reactors for High-loading Li-S Batteries

Peng Wang^a, Yunhe Song^a, Zhenming Xu^b, Na Li^a, Jinfeng Sun^{a*}, Bo Hong^{*c}, Yanqing Lai^{*c}

1. Experimental section

1.1 Preparation of the HMCs: Briefly, 250 mg ammonium molybdate tetrahydrate ($(\text{NH}_4)_6\text{Mo}_7\text{O}_{24} \cdot 4\text{H}_2\text{O}$) and 100 mg zinc acetate dihydrate was dissolved into 70 mL deionized water under stirring at room temperature for 5 min, then, 200 mg dopamine hydrochloride was added into the above solution, after stirring 30 min, a burgundy solution was achieved. Subsequently, 150 mL absolute ethanol was added into the burgundy solution, the solution becomes orange and cloudy. After stirring 10 min, 0.05 g ammonium hydroxide was added into the above sample dropwise and the pH was adjusted to 8.5. Then the mixture was stirred for 2 h and the orange-red MPD-200 was collected by centrifugation after washed with deionized water and absolute ethanol for several times. As comparisons, different amounts of dopamine hydrochloride (100 and 300 mg) were added and the MPD-100 and MPD-300 were obtained.

1.2 Synthesis of the $\text{Mo}_x\text{C} @ \text{NC}$ spheres: The as-synthesized MPDs were thermally treated at 650 °C for 2h, and raises to 850 for 5 h with a heating rate of 5 °C min⁻¹ under Ar atmosphere, respectively. Then $\text{Mo}_x\text{C} @ \text{CN}$ microspheres were obtained. The $\text{Mo}_2\text{C} @ \text{CN}$ microspheres are prepared without zinc acetate addition in the precursor and the other synthetic route followed a similar path like $\text{Mo}_x\text{C} @ \text{NC}$ spheres.

1.3 Synthesis of the 77S/ $\text{Mo}_x\text{C} @ \text{NC}$ Spheres:

Sulfur encapsulation was performed via a melt-diffusion method. A mixture of sulfur (77 wt %) with Mo_xC@NC composites was hand-milled for 20 min and then transferred to an autoclave and heated at 155 °C for 12 h. Upon cooling, the final materials were collected as 77S/Mo_xC@NC. The 77S/Mo₂C@NC and 77S/NC composites were prepared via the same procedure as above.

1.4 Preparation of Li₂S₆ Solution:

The Li₂S₆ solution was prepared by dissolving lithium sulfide (46 mg) and sublimed sulfur (224 mg) in a molar ratio of 1:7 in 5 mL in 1,2-dimethoxyethane (DME, 99.5%, Alfa Aesar), and 1,3-dioxolane (DOL, 99.5%, Alfa Aesar) (1:1 ratio, by volume).

1.5 Adsorption test

Li₂S and sulfur with a molar ratio of 1:5 were added into a DOL/ DME mixture (1:1, v/v) and stirred overnight at 60°C. The concentration of the Li₂S₆ solution was controlled to be 0.2 mmol L⁻¹. Then 10 mg of Mo_xC@NC composite, Mo₂C@NC or NC were added to 3 mL of the above Li₂S₆ solution. The mixture was stirred and rested for 1h for observation.

1.6 Materials characterization

The morphology analyses were conducted with TEM (Nova Nano SEM 230) and TEM (Tecnai G2 20ST) coupled with an attached energy dispersive X-ray spectroscopy (EDS). Powder X-ray diffraction (XRD, Rigaku 3014) were characterized with Cu-Kα source. The sulfur content was confirmed by TGA analysis (Netzsch, STA 449C) under N₂ flow at a heating rate of 10 °C/min. The N₂ adsorption measurements were performed on ASAP 2460 analyzer (Micromeritics, USA) at 77 K. The chemical state of elements in composites was tested on X-ray photo-electron spectroscopy (XPS, ESCA LAB 250Xi).

1.7 Electrochemical Measurement:

To prepare the working electrode, a slurry was obtained by mixing and stirring the as-prepared composites, conductive carbon black and polyvinylidene fluoride (PVDF)

with the mass ratio of 8:1:1 in N-methyl-2-pyrrolidone, respectively. Then, the slurry was spread onto Al current collector and dried under vacuum at 60 °C for 12 h in vacuum for 10 h. The sulfur loading was controlled at 1.9–4.9 mg cm⁻². The coin-type cells (2032) were assembled with metallic Li as the counter electrodes and Celgard 2400 as a separator. The electrolyte consisted of 1.0 m lithium bis(trifluoromethanesulfonyl) imide (LiTFSI) in 1, 3-dioxolane (DOL) and 1,2-dimethoxyethane (DME) (v/v, 1:1) with 2 % LiNO₃ as the additive. The volume of the electrolyte used in each cell was 30–50 μL, and the electrolyte-to-sulfur (E/S) ratio was about 15–20 μL mg⁻¹. Discharge/charge tests were carried out between 1.7 and 2.8 V (vs Li/Li⁺) at various C rates (1 C = 1675 mA h g⁻¹) with LAND-CT2001A instruments (Wuhan Jinnuo, China). CV and EIS measurements were performed on electrochemical workstation (Solartron 1470E battery test) with a scan rate of 0.1 mV s⁻¹. In addition, EIS were performed using electrochemical workstation (Solartron 1470E battery test) in the frequency range between 10 mHz and 100 kHz.

1.8 Computational method and models

All calculations were carried out by using the projector augmented wave method in the framework of the density functional theory (DFT)¹, as implemented in the QUANTUM ESPRESSO². The generalized gradient approximation (GGA) and Perdew–Burke–Ernzerhof (PBE) exchange functional¹ was used. The plane-wave energy cutoff was set to 38 Ry, and the Monkhorst–Pack method³ is employed for the Brillouin zone sampling. The convergence criteria of energy and force calculations were set to 10⁻⁵ Ry/atom and 0.01 Ry/Å, respectively. To explore the interactions between the polysulfide molecule and Mo₂C surfaces, the adsorption energies of the polysulfide molecule (Li₂S, Li₂S₂, Li₂S₄, Li₂S₆, Li₂S₈ and S₈) on the Mo₂C surfaces were calculated. The pure Mo₂C (101) surface was built by the 2×1 supercell with more than four atomic layers. A vacuum region of 15 Å is applied to avoid interactions between the neighboring configurations⁴. DFT-D2 method was used to account for the vdW interactions between organic molecule and Mo₂C surface⁵. Here, the adsorption energies (E_a) were calculated by the energy difference of the system

after and before adsorption⁶:

$$E_a = E(\text{polysulfide-Mo}_x\text{C}) - E(\text{polysulfide}) - E(\text{Mo}_x\text{C}),$$

where $E(\text{polysulfide-Mo}_x\text{C})$, $E(\text{polysulfide})$, and $E(\text{Mo}_x\text{C})$ represent the DFT energies of the polysulfide molecule adsorbed Mo_xC surface, the energy of an isolated polysulfide molecule, and the energy of the clean Mo_xC (101) surface.

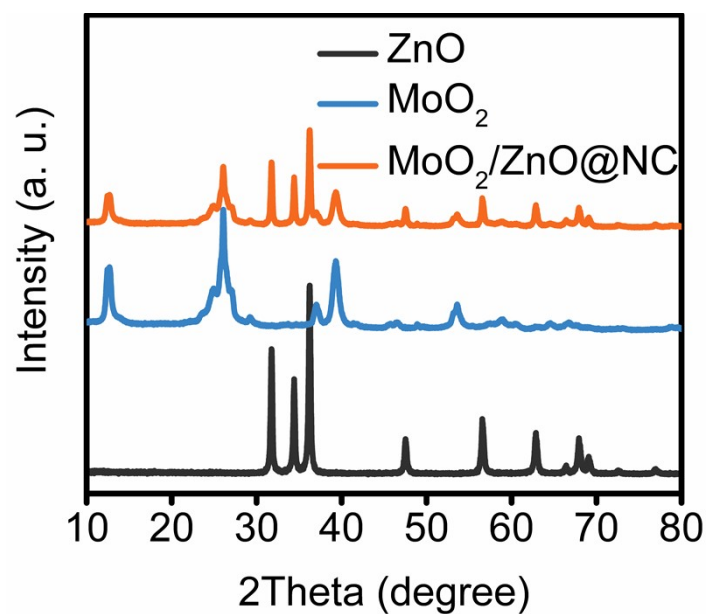


Figure S1 XRD patterns off MoO₂/ZnO@NC, MoO₂ and ZnO

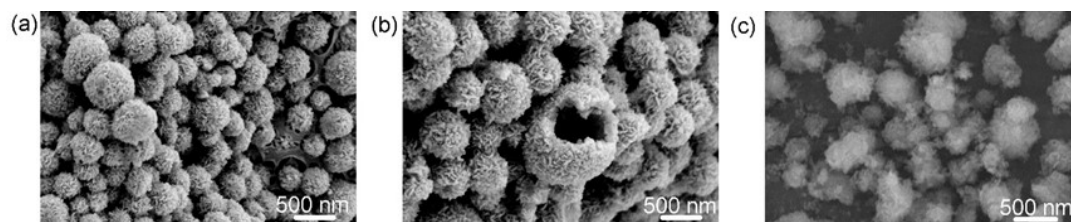


Figure S2 Typical SEM and images of the precursor. a) with 100 mg dopamine hydrochloride; b) 200 mg dopamine hydrochloride; c) 300 mg dopamine hydrochloride

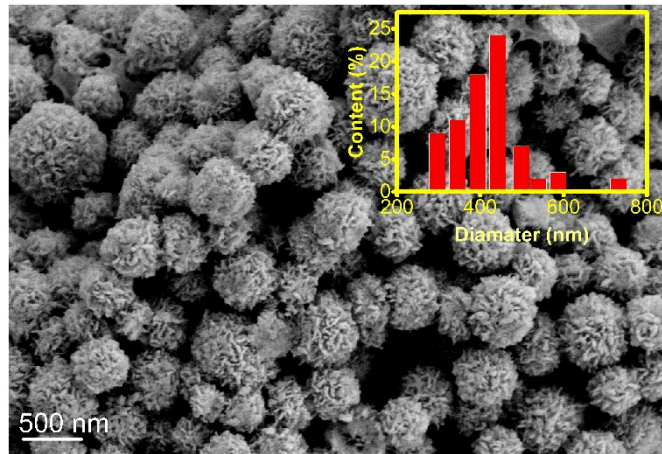


Figure S3 SEM image of $\text{Mo}_x\text{C@NC-2}$ and the corresponding particle size distribution

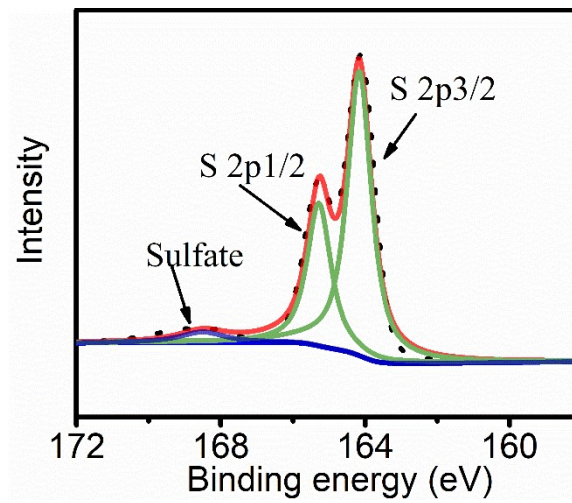


Figure. S4 XPS spectra of S 2p of the 77S/ $\text{Mo}_x\text{C@NC-2}$ composites.

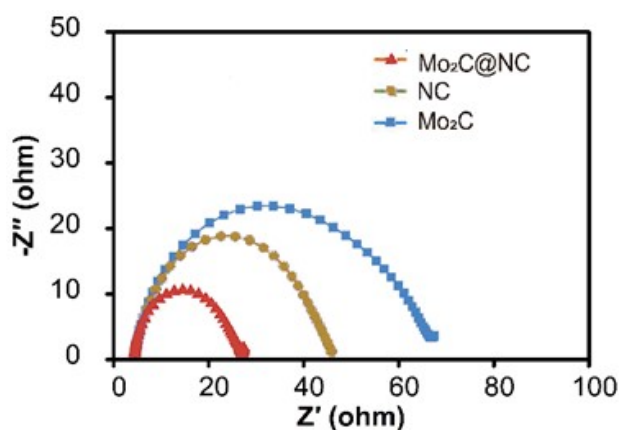


Figure S5 EIS spectral profiles recorded for symmetric cell fabricated with $\text{Mo}_x\text{C@NC}$, $\text{Mo}_2\text{C@NC}$ and NC

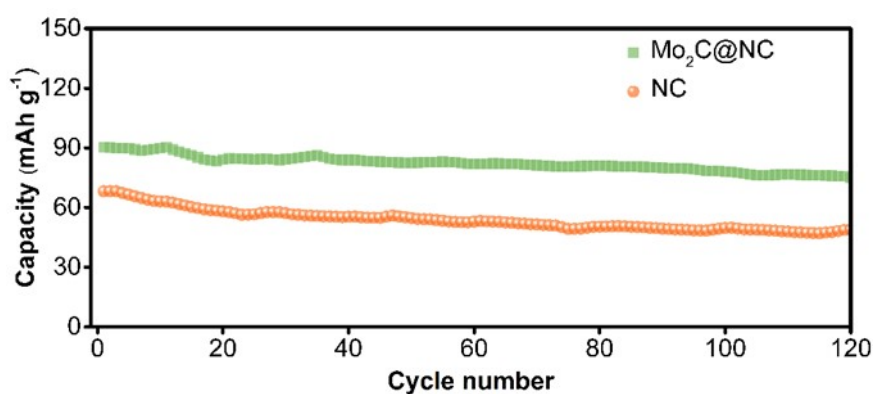


Figure S6. Long-term cycling performance of the $\text{Mo}_x\text{C@NC-2}$ and NC electrodes. (Current density= 837 mA g^{-1})

The maximum capacity that Mo_xC nanoparticles was expected to contribute by their Li^+ intercalation pseudo-capacitive behavior is calculated according to the specific capacity of $\text{Mo}_x\text{C} \times (\text{Mo}_x\text{C/S ratio of the 77S}/\text{Mo}_x\text{C@NC-2 electrode})$

For example,

The specific capacity of $\text{Mo}_2\text{C}=85 \text{ mA h g}^{-1}$,

$\text{Mo}_x\text{C}/\text{S}$ ratio of the $\text{Mo}_x\text{C}/\text{CN}^*\text{Mo}_x\text{C}/\text{S}$ cathode = $(0.31 \times 0.12) / 0.77 = 0.048$

The increased specific capacity of sulfur contributed by Mo_xC in the $77\text{S}/\text{Mo}_x\text{C}@\text{NC}-2$ cathode = $90 \times 0.043 = 5.1 \text{ mA h g}^{-1}$.

The NC deliver more than 64 mA h g^{-1} , should because the pseudo-capacitive Li^+ storage behaviour. It should be noted that after the sulfur impregnation, the surface of carbon framework should be covered by the sulfur, thus the electronic double layer capacitance (EDLC) of NC should be heavily discounted. Considering the Li^+ insertion-desertion redox reaction, the pseudo-capacitive-type capacity of Mo_2C shall not be affected. But it only contributes less than 0.48% of overall capacity.

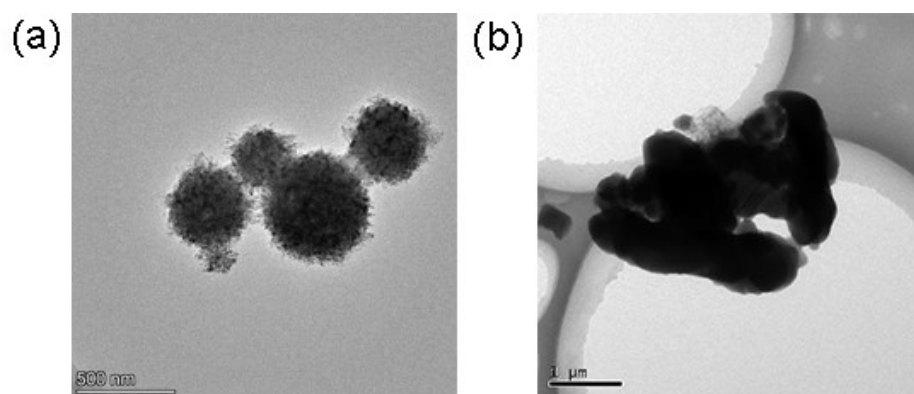


Figure S7 TEM of Mo_xC@NC-1 and Mo_xC@NC-3

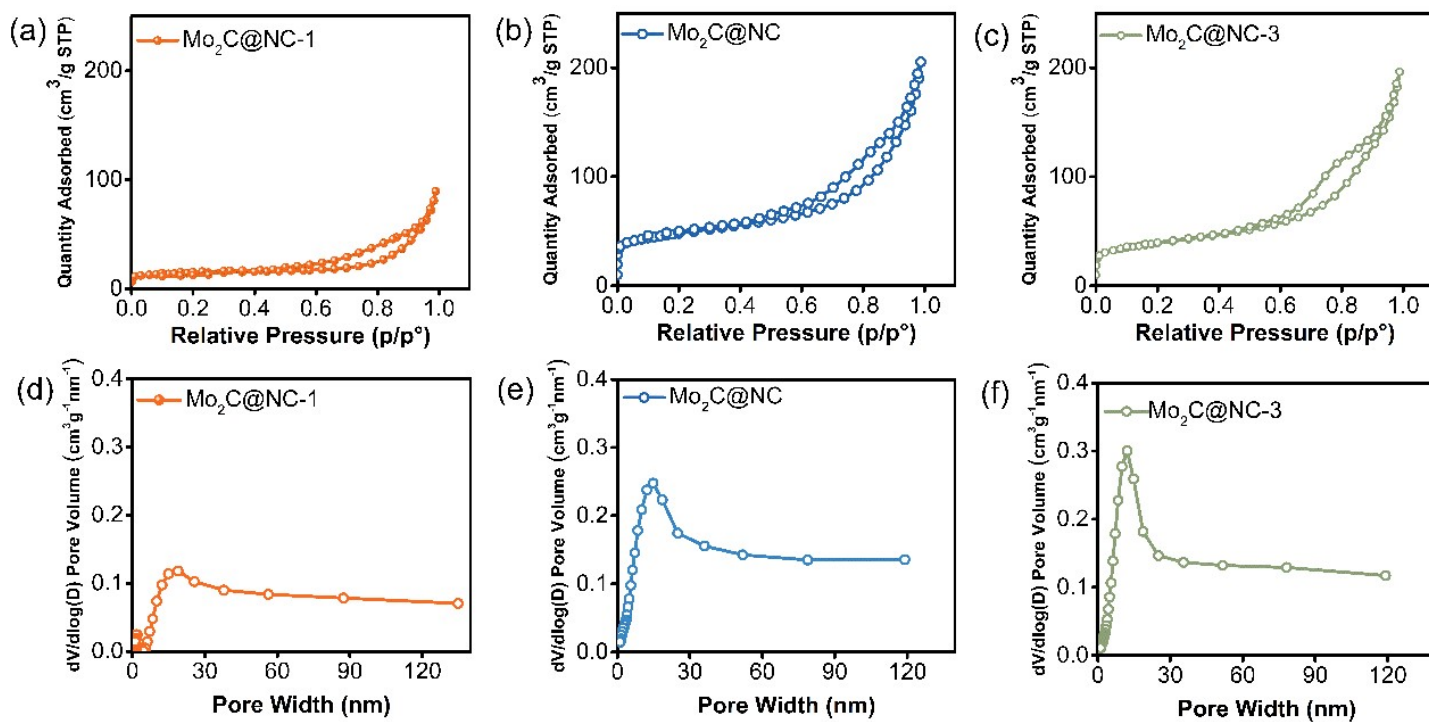


Figure S8 The N₂ adsorption-desorption curves (a, b, c) and the pore width distributions of (d, e, f) of Mo_xC@NC-1, Mo_xC@NC-2 and Mo_xC@NC-3

References

1. Kohn, W.; Sham, L. J., Self-Consistent Equations Including Exchange and Correlation Effects. *Phys. Rev.* 1965, 140 (4A), A1133-A1138.
2. Giannozzi, P.; Baroni, S.; Bonini, N.; Calandra, M.; Car, R.; Cavazzoni, C.; Ceresoli, D.; Chiarotti, G. L.; Cococcioni, M.; Dabo, I.; Dal Corso, A.; de Gironcoli, S.; Fabris, S.; Fratesi, G.; Gebauer, R.; Gerstmann, U.; Gougoussis, C.; Kokalj, A.; Lazzeri, M.; Martin-Samos, L.; Marzari, N.; Mauri, F.; Mazzarello, R.; Paolini, S.; Pasquarello, A.; Paulatto, L.; Sbraccia, C.; Scandolo, S.; Sclauzero, G.; Seitsonen, A. P.; Smogunov, A.; Umari, P.; Wentzcovitch, R. M., QUANTUM ESPRESSO: a modular and open-source software project for quantum simulations of materials. *J Phys Condens Matter* 2009, 21 (39), 395502.
3. Monkhorst, H. J.; Pack, J. D., Special points for Brillouin-zone integrations. *Physical Review B* 1976, 13 (12), 5188-5192.
4. Xu, Z.; Zhu, H., Two-dimensional manganese nitride monolayer with room temperature rigid ferromagnetism under strain. *The Journal of Physical Chemistry C* 2018, 122 (26), 14918-14927.
5. Grimme, S. A., J.; Ehrlich, S.; Krieg, H. A, Consistent and Accurate ab Initio Parametrization of Density Functional Dispersion Correction (DFT-D) for the 94 Elements H-Pu. *J. Chem. Phys* 2010, 132, 154104.
6. Lv, X.; Xu, Z.; Li, J.; Chen, J.; Liu, Q., Investigation of fluorine adsorption on nitrogen doped MgAl₂O₄ surface by first-principles. *Appl. Surf. Sci.* 2016, 376, 97-104.